

RESEARCH ARTICLE

Alzheimer's Disease Risk Polymorphisms Regulate Gene Expression in the *ZCWPW1* and the *CELF1* Loci

Celeste M. Karch^{1,2*}, Lubov A. Ezerskiy¹, Sarah Bertelsen³, Alzheimer's Disease Genetics Consortium (ADGC)[¶], Alison M. Goate^{3*}

1 Department of Psychiatry, Washington University School of Medicine, St. Louis, Missouri, United States of America, **2** Hope Center Program on Protein Aggregation and Neurodegeneration, Washington University School of Medicine, St. Louis, Missouri, United States of America, **3** Department of Neuroscience, Icahn School of Medicine at Mount Sinai, 1425 Madison Avenue, New York, NY 10029, United States of America

¶ Membership of the Alzheimer's Disease Genetics Consortium is provided in the Acknowledgments.

* karchc@psychiatry.wustl.edu (CMK); alison.goate@mssm.edu (AMG)



CrossMark
click for updates

OPEN ACCESS

Citation: Karch CM, Ezerskiy LA, Bertelsen S, Alzheimer's Disease Genetics Consortium (ADGC), Goate AM (2016) Alzheimer's Disease Risk Polymorphisms Regulate Gene Expression in the *ZCWPW1* and the *CELF1* Loci. *PLoS ONE* 11(2): e0148717. doi:10.1371/journal.pone.0148717

Editor: Qingyang Huang, Central China Normal University, CHINA

Received: October 26, 2015

Accepted: December 17, 2015

Published: February 26, 2016

Copyright: © 2016 Karch et al. This is an open access article distributed under the terms of the [Creative Commons Attribution License](https://creativecommons.org/licenses/by/4.0/), which permits unrestricted use, distribution, and reproduction in any medium, provided the original author and source are credited.

Data Availability Statement: All relevant data are within the paper and its Supporting Information files.

Funding: Funding was provided by NIH-AG035083 (AMG), NIH-AG049508 (AMG) NIH-AG046374 (CMK), and the Barnes Jewish Foundation (AMG). This work was supported by access to equipment made possible by the Hope Center for Neurological Disorders, and the Departments of Neurology and Psychiatry at Washington University School of Medicine. The funders had no role in study design, data collection and analysis, decision to publish, or preparation of the manuscript.

Abstract

Late onset Alzheimer's disease (LOAD) is a genetically complex and clinically heterogeneous disease. Recent large-scale genome wide association studies (GWAS) have identified more than twenty loci that modify risk for AD. Despite the identification of these loci, little progress has been made in identifying the functional variants that explain the association with AD risk. Thus, we sought to determine whether the novel LOAD GWAS single nucleotide polymorphisms (SNPs) alter expression of LOAD GWAS genes and whether expression of these genes is altered in AD brains. The majority of LOAD GWAS SNPs occur in gene dense regions under large linkage disequilibrium (LD) blocks, making it unclear which gene(s) are modified by the SNP. Thus, we tested for brain expression quantitative trait loci (eQTLs) between LOAD GWAS SNPs and SNPs in high LD with the LOAD GWAS SNPs in all of the genes within the GWAS loci. We found a significant eQTL between rs1476679 and *PILRB* and *GATS*, which occurs within the *ZCWPW1* locus. *PILRB* and *GATS* expression levels, within the *ZCWPW1* locus, were also associated with AD status. Rs7120548 was associated with *MTCH2* expression, which occurs within the *CELF1* locus. Additionally, expression of several genes within the *CELF1* locus, including *MTCH2*, were highly correlated with one another and were associated with AD status. We further demonstrate that *PILRB*, as well as other genes within the GWAS loci, are most highly expressed in microglia. These findings together with the function of *PILRB* as a DAP12 receptor supports the critical role of microglia and neuroinflammation in AD risk.

Introduction

Late onset Alzheimer's disease (LOAD) is a complex, heterogeneous disease with a strong genetic component (reviewed in [1]). *APOEε4* is the strongest genetic risk factor for LOAD:

Competing Interests: The authors have declared that no competing interests exist.

carrying one copy of *APOEε4* increases AD risk by 3 fold and carrying two copies of *APOEε4* increases AD risk by 8–10 fold (reviewed in [2]). However, only 50% of LOAD cases carry an *APOEε4* allele, suggesting that other genetic factors contribute to risk for LOAD.

In the last six years, genome wide association studies (GWAS) have facilitated the analysis of millions of single nucleotide polymorphisms (SNPs) in tens of thousands of samples [3–10]. The International Genomics of Alzheimer's Project (IGAP) has recently applied this approach to LOAD case and control studies in 74,046 individuals, revealing 21 loci that modify LOAD risk: *ABCA7*, *APOE*, *BIN1*, *CASS4*, *CD2AP*, *CD33*, *CELF1*, *CLU*, *CRI*, *EPHA1*, *FERMT2*, *HLA-DRB5/DRB1*, *INPP5D*, *MEF2C*, *MS4A6A*, *NME8*, *PICALM*, *PTK2B*, *SLC24A4*, *SORL1*, and *ZCWPW1* [9]. The IGAP GWAS genes fall into several common pathways that have been previously implicated in AD: neural development, synapse function, endocytosis, immune response, axonal transport, and lipid metabolism (reviewed in [1]). However, the specific effects of these SNPs on gene function and the resulting impact on disease remains poorly understood [11–14]. Two aspects of GWAS approaches have limited the interpretations that we can make regarding the functional impact of these SNPs on the molecular mechanisms underlying AD. First, the majority of the most significant GWAS SNPs are located in non-coding or gene-dense regions, making it challenging to identify which gene the SNP is modifying. Second, the majority of GWAS top SNPs are in high linkage disequilibrium (LD) with many SNPs, which in some cases span hundreds of kilobases, making it difficult to determine which SNP is the functional variant responsible for modifying LOAD risk.

Our group and others have previously demonstrated that some LOAD GWAS genes are differentially expressed in AD brains [11, 15, 16]. We found that expression levels of some LOAD GWAS genes that were identified in early GWAS [3–8], including *ABCA7*, *BIN1*, *CD33*, *CLU*, *CRI*, and *MS4A6E*, are associated with clinical and/or neuropathological aspects of AD [15] but failed to identify strong expression quantitative trait loci (eQTLs) [15, 17].

Despite the identification of additional, novel GWAS loci that modulate LOAD risk, we still know little of the functional impact of LOAD GWAS SNPs and the role of these genes in AD pathogenesis. We sought to examine functional effects of IGAP GWAS SNPs by examining eQTLs in several human brain expression cohorts. To do this, we identified all of the genes that fell within the LD block for each IGAP GWAS locus. We then analyzed eQTLs and association with AD status. rs1476679 and rs7120548 are associated with *PILRB* and *MTCH2* expression, respectively. Additionally, the expression of several genes within the *CELF1* locus, including *MTCH2*, were highly correlated and were associated with AD status. Importantly, these significant eQTLs and expression differences in LOAD brains were observed in genes that occur within the IGAP GWAS loci but not the named IGAP GWAS gene. Together, our findings demonstrate that several LOAD risk variants modify expression of nearby genes and may contribute to LOAD risk.

Results

Identifying genes associated with IGAP GWAS SNPs

A recent IGAP GWAS in 74,046 individuals revealed 21 loci that are significantly associated with altered AD risk, 12 of which are novel [9]: *ABCA7*, *APOE*, *BIN1*, *CASS4*, *CD2AP*, *CD33*, *CELF1*, *CLU*, *CRI*, *EPHA1*, *FERMT2*, *HLA-DRB5/DRB1*, *INPP5D*, *MEF2C*, *MS4A6A*, *NME8*, *PICALM*, *PTK2B*, *SLC24A4*, *SORL1*, and *ZCWPW1*. To define the functional impact of the IGAP SNPs, we used RegulomeDB and HaploReg to predict the regulatory potential of the IGAP SNPs (S1 Table) [18]. One IGAP SNP, rs1476679, produced a RegulomeDB score with suggestive regulatory potential (Score: 1f; Table 1) [19]. RegulomeDB predicts that rs1476679 affects protein binding of RFX3, FOS and CTCF and exhibits eQTLs with *GATS*, *PILRB*, and

Table 1. Regulatory effects of IGAP top SNPs.

IGAP Gene	IGAP SNP	Score	RegulomeDB			HaploReg		
			eQTL	Motif Changed	Proteins Bound	eQTL	Motifs Changed	Proteins Bound
ZCWPW1	rs1476679	1f	<i>TRIM4</i> , <i>PILRB</i> , <i>GATS</i> *	-	CTCF, FOS, RFX3	-	-	CTCF
DSG2	rs8093731	2b	-	PAX6	E2F4, FOS	-	AHR, NKX2, NKX3, PAX6, PBX3	-
PICALM	rs10792832	3a	-	FAC1	SPI1	-	AP-3, FAC1, HDAC2	-
MS4A6A	rs983392	4	-	-	RUNX1	-	HMG-IY, HAND1, MYC	-
ABCA7	rs4147929	4	-	-	MAZ, IRF1	-	HNF4,SP2	-
CR1	rs6656401	5	-	-	-	-	RXRA,YY1	-
BIN1	rs6733839	5	-	MEF2, PU.1	-	-	DOBOX4, MEF2, NFκB, VDR	-
EPHA1	rs11771145	5	-	-	-	-	HOXD10	GATA2
CLU	rs9331896	5	-	-	-	-	BDP1, NRSF	-
CD33	rs3865444	5	-	-	-	-	CDP, FOXO, SREBP	-
HLA	rs9271192	5	-	-	CHD1, MXI1, TBP	-	HOXA13, POU2F2, TCF11::MAFG	POL2
PTK2B	rs28834970	5	-	-	-	-	CEBPA, CEBPB, CEBPD, HSF,STAT, P300	-
SORL1	rs11218343	5	-	-	POLR2A, TBP, RFX3	-	-	-
SLC24A4/ RIN3	rs10498633	5	-	-	-	-	AP1, CDX2, FOXD1, FOXJ2, HOXA9, HOXC10, HOXC9, MRG1:HOXA9, NKX6, PDX1, TCF12, P300	-
INPP5D	rs35349669	5	-	RBP-Jκ	-	-	AP-2rep,RBP-Jκ	-
FERMT2	rs17125944	5	-	-	-	-	PU.1, SRF, P300	-
CASS4	rs7274581	5	-	-	-	-	E2F, SIN3AK-20, YY1	-
CD2AP	rs10948363	6	-	FOXJ3, TCF3	-	-	FOXJ1, HOXB13, SOX	-
CELF1	rs10838725	6	-	C/EBPΔ, FOXA2, HNF3β	-	-	CEBPB, CEBPD, Foxa	-
MEF2C	rs190982	7	-	-	-	-	GATA, HNF1	-
NME8	rs2718058	7	-	-	-	-	AP1, ELF3, FOXA, HMG-IY, MEF2, PAX6, STAT	-

*Monocytes. PU.1 is the protein product of SPI1

doi:10.1371/journal.pone.0148717.t001

TRIM4 (Table 1). Rs8093731 modifies a PAX6 motif and protein binding of E2F4 and FOS (Score: 2b; Table 1). Rs10792832 modifies an *FAC1* motif and binding of SPI1 (Score: 3a; Table 1). Despite the identification of several SNPs that have suggestive regulatory potentials, we were unable to identify eQTLs in either RegulomeDB or HaploReg that occur within the named LOAD GWAS gene (Table 1).

The majority of GWAS SNPs occur in regions of high LD that span multiple genes [9]. Thus, we asked whether IGAP GWAS SNPs alter expression of genes that are within the LD block rather than the genes immediately under the SNP with the highest p-value. Manhattan plots reported in Lambert et al. were used to identify all of the genes within the LD block for each IGAP GWAS SNP (Table 2) [9]. Eleven of the 21 IGAP GWAS SNPs have multiple genes within the LD block. We tested whether the IGAP GWAS SNPs have functional effects on gene expression by examining all of the genes within each region.

Table 2. Genes within the IGAP GWAS loci.

IGAP SNP	IGAP Gene	Genes within LD block
rs6656401	<i>CR1</i>	<i>CR2, CR1L</i>
rs6733839	<i>BIN1</i>	<i>CYP27C1</i>
rs10948363	<i>CD2AP</i>	None
rs11771145	<i>EPHA1</i>	<i>LOC285965, TAS2R60</i>
rs9331896	<i>CLU</i>	None
rs983392	<i>MS4A6A</i>	<i>MS4A3, MS4A2, MS4A6A, MS4A4A, MS4A6E</i>
rs10792832	<i>PICALM</i>	<i>EED</i>
rs4147929	<i>ABCA7</i>	<i>CNN2, POLR2E, GPX4, HMHA1, SBNO2</i>
rs3865444	<i>CD33</i>	None
rs9271192	<i>HLA-DRB5– HLA-DRB1</i>	<i>HLA-DRB6, HLA-DQA1, HLA-DQB1</i>
rs28834970	<i>PTK2B</i>	None
rs11218343	<i>SORL1</i>	None
rs10498633	<i>SLC24A4 & RIN3</i>	None
rs8093731	<i>DSG2</i>	<i>DSG3</i>
rs35349669	<i>INPP5D</i>	None
rs190982	<i>MEF2C</i>	None
rs2718058	<i>NME8</i>	<i>GPR141</i>
rs1476679	<i>ZCWPW1</i>	<i>NYAP1, PMS2P1, PILRB, PILRA, C7ORF61, C7ORF47, MEPCE, GATS</i>
rs10838725	<i>CELF1</i>	<i>MADD, SLC39A13, PSMC3, NDUFS3, KBTBD4, PTPMT1, MTCH2, AGBL2, FNBP4, NUP160, C1QTNF4, RAPSN</i>
rs17125944	<i>FERMT2</i>	None
rs7274581	<i>CASS4</i>	<i>C20ORF43, CSTF1</i>

doi:10.1371/journal.pone.0148717.t002

eQTLs in AD Risk Loci

To determine whether IGAP GWAS SNPs modify expression of genes within the GWAS loci, we examined cis-eQTLs in a publicly available dataset from neuropathologically confirmed normal control brains (UKBEC [20]; Table 3 and S2 Table). Rs1476679 was significantly associated with expression of multiple *PILRB* transcripts in most brain regions (Table 3). Several transcripts shared between *PILRB* and *PILRA* were associated with rs1476679. However, transcripts specific to *PILRA* did not exhibit an eQTL with rs1476679, suggesting that the effect is driven by differences in *PILRB* specifically (Table 3). *GATS*, which is also present within the LD block of the IGAP SNP, had a single transcript that also displayed an eQTL with rs1476679 in most brain regions (Table 3). The IGAP SNP, rs9331896, was significantly associated with *CLU* expression in the white matter, hippocampus, temporal cortex and occipital cortex (Table 3). EQTLs were also observed between rs6656401 and *CR1*, *CR2* and *CR1L*, all of which occur within the LD block for rs6656401. The IGAP SNP rs10838725, occurs in a gene dense region and several genes within this region exhibited eQTLs with the IGAP SNP: *CELF1*, *NDUF3*, *KBTBD4*, *PTPMT1*, *MTCH2*, *FNBP4*, *MADD* and *NUP160* (Table 3). IGAP SNPs rs983392, rs10792832, rs2718058, and rs7274581 exhibited eQTLs with *MS4A6A*, *EED*, *GPR141*, and *CASS4*, respectively (Table 3). Although several loci showed nominal association, only the *CR1* eQTL in WHMT survived a strict multiple test correction (Bonferroni $p = 3.9 \times 10^{-5}$).

Our initial analyses were performed using the candidate genes manually selected from genes within the IGAP GWAS loci. We next applied an unbiased approach to determine which genes are most highly associated with the IGAP GWAS SNPs (UKBEC; S3 Table). A subset of the

Table 3. (Continued)

IGAP SNP	Gene	Transcript	Probe ID	Brain Region (P value)											
				FCTX	TCTX	HIPP	PUTM	THAL	MEDU	SNIG	WHMT	CRBL	OCTX		
	<i>KBTD4</i>	t3372337	3372347	0.75	0.91	0.93	0.70	0.90	0.76	1.00	0.16	1.10x10⁻³	0.82		
	<i>PTPMT1</i>	t3372006	3372066	0.86	7.90x10⁻³	0.12	0.67	0.55	0.04	1.00	0.84	0.90	0.96		
			3372037	0.86	0.14	0.74	0.67	6.70x10⁻³	0.02	0.78	0.10	0.40	0.19		
			3372007	0.92	0.13	0.14	0.46	0.07	0.26	0.29	0.72	2.50x10⁻³	0.34		
			3372006	0.31	0.77	0.68	0.93	0.31	9.10x10⁻⁴	0.65	0.98	0.61	0.39		
	<i>MTCH2</i>	t3372368	3372370	0.78	9.50x10⁻³	0.06	0.32	7.20x10⁻³	1.40x10⁻³	0.60	0.13	0.17	0.20		
	<i>FNBP4</i>	t3372459	3372495	0.79	0.67	0.51	0.41	1.30x10⁻³	3.30x10⁻³	0.66	0.16	0.40	0.10		
			3372515	0.56	0.22	5.10x10⁻⁴	0.94	0.03	0.16	0.83	0.07	0.77	2.90x10⁻⁴		
			t3372459	0.96	0.43	0.86	0.72	3.90x10⁻³	3.60x10⁻⁴	0.66	0.24	0.95	0.13		
	<i>NUP160</i>	t3371986	3372006	0.31	0.77	0.68	0.93	0.31	9.10x10⁻⁴	0.65	0.98	0.61	0.39		
	<i>SLC39A13</i>						No eQTL								
	<i>PSMC3</i>						No eQTL								
	<i>AGBL2</i>						No eQTL								
	<i>C1QTNF4</i>						No eQTL								
	<i>RAPSN</i>						No eQTL								

*IGAP Gene. No eQTL indicates p value was greater than 0.05 in all brain regions. P values reported for all IGAP SNPs and genes within each loci in Supplemental Table 2. Bonferroni p = 3.9x10⁻⁵

doi:10.1371/journal.pone.0148717.t003

Table 4. SNPs in LD with rs1476679 produce eQTL with *PILRB* in control brains (GSE15745).

Analyzed SNP	PILRB Transcript	Frontal Cortex		Temporal Cortex	
		P value	β	P value	β
rs5015756	ILMN_1768754	0.2952	0.0375	0.0182	0.1035
	ILMN_1685534	5.65x10^{-5*}	0.0678	0.0572	0.0274
	ILMN_1723984	3.26x10^{-5*}	0.0811	4.12x10^{-5*}	0.0575
	ILMN_1760345	0.0384	0.0462	0.4359	0.0101
	ILMN_1729915	0.7101	-0.0046	0.5242	0.0084
	ILMN_1663753	0.0732	0.0213	0.0257	0.0309

* Passed multiple test correction (Bonferroni $p = 3.2 \times 10^{-4}$)

doi:10.1371/journal.pone.0148717.t004

Table 5. eQTLs of IGAP GWAS SNPs in GSE15222.

IGAP SNP	IGAP Gene	Analyzed SNP	Gene	P value	β
rs1476679	<i>ZCWPW1</i>	rs1476679	<i>PILRB</i>	0.0022	0.108811
rs10838725	<i>CELF1</i>	rs7120548	<i>MTCH2</i>	0.0011	0.07507

doi:10.1371/journal.pone.0148717.t005

IGAP SNPs, rs6656401, rs9331896, rs28834970, and rs10498633, and rs190982, were associated with expression of the named IGAP gene, *CRI*, *CLU*, *PTK2B*, *SLC24A4*, and *MEF2C*, respectively (S3 Table). For the majority of the IGAP SNPs, genes that occur within the LD block for the IGAP GWAS loci are among the ten most highly associated eQTLs; however, the associations failed to achieve statistical significance (S3 Table).

In order to replicate these eQTL findings, we analyzed a second publically available dataset composed of expression and genotype information from neuropathologically normal control brains (GSE15745 [21]). In most cases, the original GWAS SNP was not present in the dataset; so, we used one or more SNPs in high LD with the GWAS SNP to test for eQTLs (Table 4; S4 Table). Cis-eQTLs were analyzed in frontal and temporal cortices (Table 4; S4 Table). We observed a significant association between rs5015756, in LD with IGAP SNP rs1476679 ($r^2 = 0.8$; $D' = 1$; S5 Table), and several *PILRB* probes (Table 3; $p = 3.26 \times 10^{-5}$, FCTX, and 4.12×10^{-5} , TCTX; Bonferroni $p = 3.2 \times 10^{-4}$).

In a third replication dataset containing expression and genotype information from AD and control brains (GSE15222), we were able to replicate the eQTL between rs1476679 and *PILRB* ($p = 0.0022$; Table 5; Bonferroni $p = 0.003$). Additionally, we replicated the eQTL observed in the UKBEC dataset between rs7120548 and *MTCH2*, a gene located in the *CELF1* locus ($p = 0.0011$; Table 5) [22]. In GSE15222, very few genes were present in the cleaned dataset that occur within the GWAS loci for the IGAP SNPs (e.g. *CLU* and *CRI*), making it impossible to independently replicate a subset of eQTLs (S6 Table).

Thus, three independent datasets demonstrate that rs1476679 is associated with altered *PILRB* expression in multiple brain regions. Additionally, these datasets provide evidence for a much more complex picture of AD genetic risk than was previously reported in the original IGAP GWAS: (1) the majority of IGAP GWAS SNPs do not significantly affect expression of nearby genes in brain homogenates and (2) eQTLs occur in genes that are near the IGAP SNP but not that have been named as an IGAP gene.

Identifying the most significant eQTL SNP within IGAP GWAS loci

Because the majority of GWAS top SNPs are in high LD with many SNPs, it is difficult to determine which SNP is the functional variant responsible for modifying LOAD risk. To determine whether other SNPs within the IGAP GWAS loci more significantly contribute to eQTLs, we identified all SNPs within the IGAP GWAS loci with a p-value of 10^{-5} or lower [9]. We then used an unbiased approach to determine which genes are most highly associated with the SNPs within the IGAP GWAS loci (UKBEC; [S7](#) and [S8](#) Tables). Assuming the most stringent cut-off for multiple test correction ($p = 10^{-6}$) [20], we identified SNPs within the *CR1*, *ZCWPW1*, *CLU*, and *PTK2B* loci that produced significant eQTLs ([S7 Table](#)).

To determine whether the SNPs that produce the most significant eQTL within each IGAP GWAS locus represent the same signal as the GWAS top SNP or an independent signal, we tested for the association of the IGAP GWAS top SNP with AD risk and then conditioned the analysis based on the most significant eQTL SNP within each locus ([S9 Table](#)). Using this approach, in the ADGC subset of the IGAP dataset, we found that for each locus, the most significant eQTL SNP and the IGAP top SNP represented the same signal. Thus, while we identified SNPs within IGAP GWAS loci that produce stronger eQTLs than the IGAP top SNP, these SNPs are likely marking a single risk locus.

Expression differences in AD brains

To determine whether the named LOAD GWAS genes or genes within the GWAS loci exhibit altered expression in AD brains, we examined gene expression in a study of laser micro-dissected neurons (GSE5281; [Table 6](#)). *MTCH2* expression was significantly associated with AD status, where expression levels were lower in AD cases compared with controls ($p = 2.2 \times 10^{-12}$ and 2.9×10^{-12} ; [Table 6](#); Bonferroni $p = 5 \times 10^{-4}$). *PILRB* expression was also associated with disease status, where *PILRB* expression was lower in AD cases compared with controls ($p = 1.2 \times 10^{-3}$; [Table 6](#)). Expression of *GATS*, also within the *ZCWPW1* locus, was associated with AD status in the same direction as *PILRB* ($p = 2.1 \times 10^{-7}$; [Table 6](#)).

Several genes within the GWAS loci were associated with disease status in the neuron-specific expression dataset (GSE5281): *EED*, *POLR2E*, *GPX4*, *SORL1*, *INPP5D*, *MEF2C*, *C7ORF61*, *CELF1*, *PSMC3*, *NDUFS3*, *PTPMT1*, *NUP160*, *C20ORF43*, and *CSTF1* ([Table 6](#); [S10 Table](#)). Interestingly, expression of several genes within the *CELF1* GWAS locus were associated with disease status: *CELF1*, *SLC39A13*, *PSMC3*, *PTPMT1*, *NDUFS3*, *MTCH2*, *FNBP4*, and *NUP160*, some of which also produced suggestive evidence of eQTLs ([Table 3](#), [S3](#) and [S4](#) Tables). Expression of *MTCH2*, *NDUFS3*, *PTPMT1*, *PSMC3*, and *NUP160* (but not *CELF1*) were highly correlated in control neurons ([Fig 1](#)), and this correlation is lost in AD brains ([Fig 1](#)). Interestingly, despite the eQTLs and disease associations with *PILRB* and *GATS* expression, there was no correlation between these genes ([S1 Fig](#)). As with our eQTL findings, very few of the genes associated with disease status were the genes originally identified as the gene associated with the IGAP top SNP.

Cell-type specific expression of genes within the GWAS loci

Evidence from multiple, independent datasets have identified eQTLs between IGAP SNPs and *PILRB* and multiple genes within the *CELF1* locus (including *MTCH2*). We have also observed altered expression levels of *PILRB* and *GATS* within the *ZCWPW1* locus and *MTCH2* and other genes within the *CELF1* locus in AD brains. This could be due to differences in expression within a cell or to differences in the numbers of cells in which these genes are expressed. To determine whether genes within the *CELF1* locus and other IGAP GWAS loci are preferentially expressed in certain cell-types in the brain, we examined a dataset containing RNAseq

Table 6. Expression of IGAP GWAS loci is associated with disease status in GSE5281.

IGAP Loci	Gene	Probe ID	P values	β	
<i>ZCWPW1</i>	<i>ZCWPW1</i>	223992_x_at	0.0261	-0.3555	
	<i>ZCWPW1</i>	220618_s_at	0.8938	0.015	
	<i>PMS2P1</i>	239699_s_at	0.1083	-0.2038	
	<i>PMS2P1</i>	214526_x_at	0.7354	-0.0258	
	<i>C7orf51</i>	1553288_a_at	0.0156	0.2291	
	<i>C7orf61</i>	229913_at	7x10⁻⁴	0.4589	
	<i>C7orf47</i>	226434_at	0.2368	0.0969	
	<i>MEPCE</i>	219798_s_at	0.3281	0.0878	
	<i>PILRA</i>	219788_at	0.2172	0.1819	
	<i>PILRA</i>	222218_s_at	0.2141	0.1406	
	<i>PILRB</i>	220954_s_at	1.2x10⁻³	-0.5226	
	<i>PILRB</i>	225321_s_at	0.0915	0.1579	
		<i>GATS</i> [#]	227321_at	2.1x10⁻⁷	-0.4098
	<i>CELF1</i>	<i>CELF1</i> [#]	1555467_a_at	3.8x10⁻⁹	-0.9599
<i>CELF1</i>		209489_at	0.1711	-0.0928	
<i>CELF1</i>		221743_at	1.5x10⁻³	0.2706	
<i>CELF1</i>		204113_at	0.4106	-0.1278	
<i>CELF1</i>		221742_at	0.317	0.1058	
<i>CELF1</i>		235297_at	0.2333	0.2114	
<i>CELF1</i>		235865_at	0.8078	0.0408	
<i>SLC39A13</i>		225277_at	3.1x10⁻³	0.2519	
<i>SLC39A13</i>		1552295_a_at	0.6693	-0.0465	
<i>PSMC3</i> [#]		201267_s_at	4.80x10⁻⁶	-0.7725	
<i>NDUFS3</i> [#]		201740_at	6.6x10⁻¹¹	-0.8212	
<i>MTCH2</i> [#]		217772_s_at	2.2x10⁻¹²	-0.6621	
<i>MTCH2</i> [#]		222403_at	2.9x10⁻¹²	-0.6235	
<i>PTPMT1</i> [#]		223808_s_at	2.9x10⁻⁷	-0.3872	
<i>PTPMT1</i> [#]		225901_at	1.2x10⁻⁵	-0.7372	
<i>PTPMT1</i>		218570_at	0.0544	-0.1777	
<i>AGBL2</i>		220390_at	0.0813	0.2846	
<i>FNBP4</i>		212232_at	3.1x10⁻³	-0.4194	
<i>FNBP4</i>		235101_at	0.0484	0.3496	
<i>FNBP4</i>		242472_x_at	0.0534	0.301	
<i>FNBP4</i>	229272_at	0.5129	-0.1087		
<i>NUP160</i> [#]	212709_at	1x10⁻⁴	0.4791		
<i>NUP160</i>	214962_s_at	0.0477	-0.3451		
<i>NUP160</i>	214963_at	0.0587	-0.3362		
<i>KBTBD4</i>	218570_at	0.0544	-0.1777		
<i>KBTBD4</i>	218569_s_at	0.0944	-0.25		
<i>KBTBD4</i>	223765_s_at	0.3863	0.1439		

[#]Passed multiple test correction (Bonferroni $p = 5 \times 10^{-4}$)

doi:10.1371/journal.pone.0148717.t006

performed in isolated cell-types in the mouse brain (http://web.stanford.edu/group/barres_lab/brain_rnaseq.html [23]). We found that genes within the *CELF1* locus are most highly expressed in non-neuronal cell-types (S11 Table). This suggests that genes within this region act cooperatively to modify AD risk.

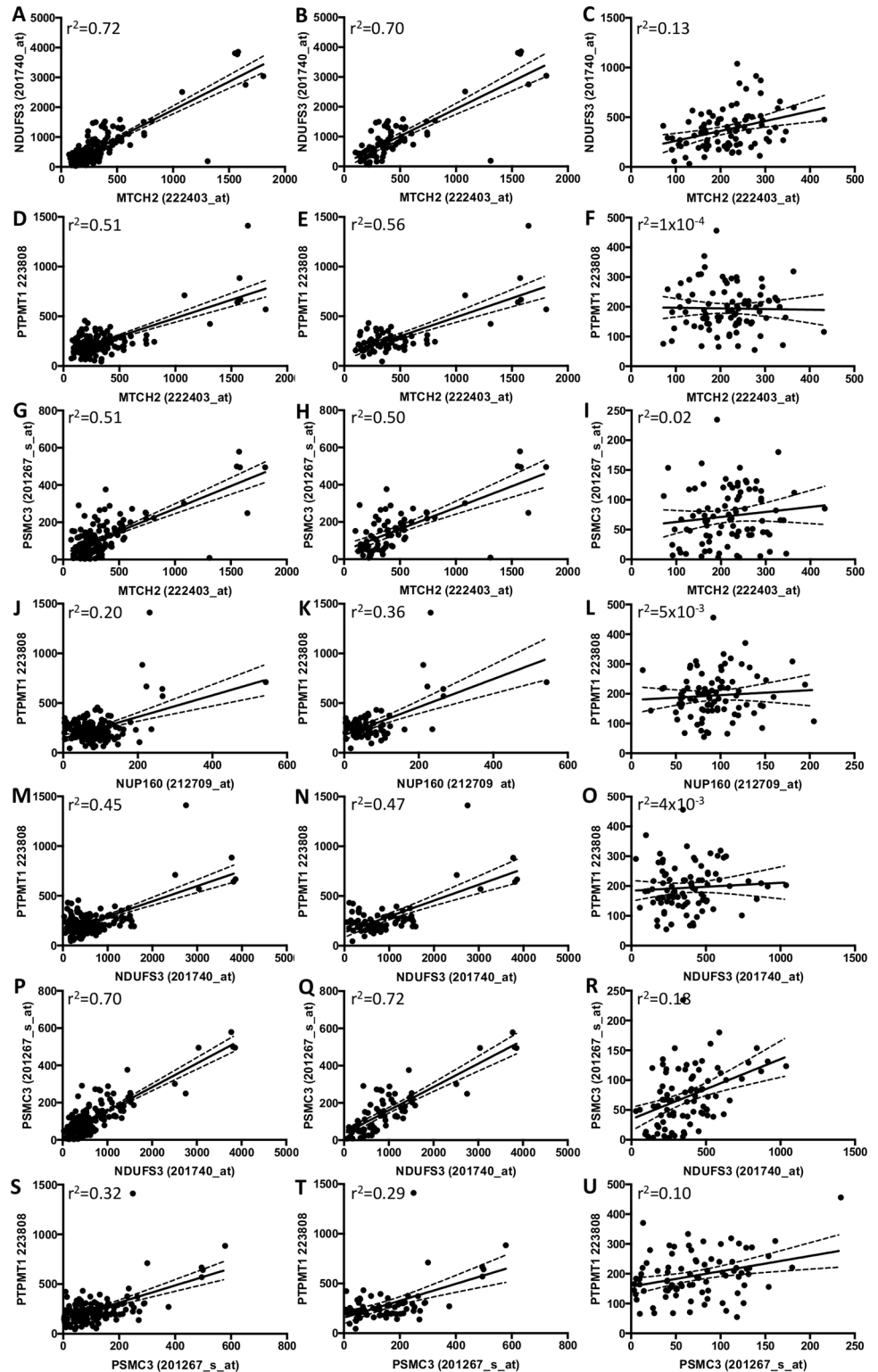


Fig 1. Correlation between expression of genes within the *CELF1* locus is lost in AD brains. Expression of *MTCH2*, *NDUFS3*, *PTPMT1*, *PSMC3*, and *NUP160* are highly correlated in laser microdissected neurons. Correlation is lost in AD brains. Gene expression in all brain samples (A, D, G, J, M, P, S). Control only (B, E, H, K, N, Q, T). AD only (C, F, I, L, O, R, U).

doi:10.1371/journal.pone.0148717.g001

We examined cell-type specific expression of all of the genes within the IGAP GWAS loci (S11 Table). We found that the majority of genes within the IGAP GWAS loci are most highly expressed in microglia (37%): *MEF2C*, *BIN1*, *PICALM*, *CD33*, *CSTF1*, *HLA-DRB1*, *HLA-DQA1*, *HLA-DQB1*, *RIN3*, *INPP5D*, *PILRA*, *SLC39A13*, *CASS4*, and *PTK2B*. To a lesser extent, genes within the IGAP GWAS loci are expressed in endothelial (20%), oligodendrocytes (20%), and astrocytes (17%). Neuronally expressed genes, which have been the central focus of functional studies regarding these and other AD risk genes, only represent 11% of IGAP GWAS loci: *ABCA7*, *MADD*, *CELF1*, and *MEF2C*. These findings provide further evidence of the complex interplay between genotype, expression, and cell-type that mediates AD risk.

Discussion

Recent studies have identified novel GWAS loci that modulate LOAD risk; however, we still know little of the functional impact of LOAD GWAS SNPs and the role of these genes in AD pathogenesis. In this study, we examined functional effects of IGAP GWAS SNPs by examining eQTLs in several human brain expression cohorts. We found that rs1476679 and rs7120548 are consistently associated with *PILRB* and *MTCH2* expression across multiple cohorts, respectively. Additionally, expression of several genes within the *CELF1* locus, including *MTCH2*, were associated with AD status. From this study, we have generated two important findings: (1) the majority of IGAP GWAS SNPs do not significantly affect expression of nearby genes in human brain homogenates and (2) eQTLs occur in genes that are near the IGAP SNP but that are not named as an AD risk gene.

PILRB is a paired immunoglobulin-like type 2 receptor that is involved in regulation of immune response [24]. *PILRB* contains highly related activating and inhibitory receptors. *PILRA* is the inhibitory counterpart to *PILRB*. *PILRB*, through activation, and *PILRA*, through inhibition, function cooperatively to control cell signaling via SHP-1, which mediates dephosphorylation of protein tyrosine residues. *PILRA* and *PILRB* are mainly expressed by cells of the myeloid lineage [24]. *PILRB* associates with DAP12, a signaling adaptor protein that is cleaved by γ -secretase and associates with TREM2, another AD risk gene [25–28]. *PILRB* also contains a sialic acid binding domain, similar to the one described for *CD33* [11, 14, 29]. Rs1476679 produced an eQTL with *PILRB* transcripts in human brain homogenates as well as in monocytes (Table 1)[30], suggesting that this AD risk SNP may influence *PILRB* expression in microglia in the brain.

One hypothesis based on our observation that multiple genes within the *CELF1* loci have eQTLs or are associated with AD status is that there is a key regulator within this region that is influencing the expression of many genes. *MTCH2* is a mitochondrial carrier protein that induces mitochondrial depolarization [31]. *MTCH2* associates with truncated BID to activate apoptosis [31]. *MTCH2* interacts with presenilin 1 [32, 33]. A second mitochondrial protein that displayed some eQTL evidence and association with disease status, *NDUFS3*, also occurs within the *CELF1* locus. *NDUFS3* is a component of the NADH-ubiquinone oxidoreductase (Complex 1). *NDUFS3* occurs in KEGG pathways for AD, Parkinson's disease, and Huntington's disease (KO05010, KO05012, KO05016). The third gene within this locus, *NUP160*, with some evidence of an eQTL and altered expression in AD brains, is a key component of the nuclear pore complex, which mediates nucleoplasmic transport. *NUP160* has an extremely long half-life and is thus susceptible to oxidative and age-related damage. Age-related defects in *NUP160* and the nuclear pore complex has been proposed to contribute to abnormal protein trafficking, and in turn to neurodegenerative diseases [34, 35]. *PTPMT1* is a lipid phosphatase that dephosphorylates mitochondria proteins, which in turn regulates mitochondrial membrane integrity. *PSMC3* encodes the 26S proteasomal subunit, which plays a critical role in

ATP-dependent degradation of ubiquitinated proteins. *MTCH2*, *NUP160*, *NDUFS3*, *PTPMT1*, and *PSMC3* expression are highly correlated in human brains and this correlation is lost in AD brains.

Our cell-type specific expression studies illustrate that the majority of the genes expressed within the IGAP GWAS loci are most highly expressed in microglia. These findings illustrate the important role of immune response and clearance in LOAD pathogenesis. This has been further supported in recent studies demonstrating that genetic variants linked with neurodegeneration are more likely to affect gene regulation in monocytes than in T cells [36].

One caveat to the study is that not all of the genes present within all of the IGAP loci were present in the cleaned expression dataset for GSE15745. Thus, we cannot exclude the possibility that other genes within the loci also have significant eQTLs with the IGAP SNPs. Most of these eQTL studies are also based on RNA extracted from brain homogenates, thus eQTLs in cells that represent a minority of cells within that tissue homogenate may not be detectable using this approach. It also remains possible that GWAS SNPs drive changes at the protein level or drive transient changes in human brains. However, our findings of several strong associations with IGAP SNPs and expression of genes that were not named as AD risk genes emphasizes that the IGAP SNPs with putative functional effects may act on genes within the GWAS loci rather than the genes immediately under the most significant IGAP SNP.

Methods

Publically available expression datasets

GSE15745. The GSE15745 dataset was obtained from control brains [21]. Brains from 150 neurologically normal individuals of European descent were obtained from the Department of Neuropathology, Johns Hopkins University, Baltimore and from the Miami Brain Bank. Brain tissue was collected from the cerebellum, frontal cortex, pons and the temporal cortex. The samples were 31.3% female with a mean age of 45.8 years (range 15–101) and an average PMI of 14.3 hours. SNP genotyping was performed on DNA extracted from cerebellar tissue for each subject using Infinium HumanHap550 version 3 BeadChips. RNA expression was measured using HumanRef-8 Expression BeadChips (Illumina). To analyze RNA expression residual values were used that were log transformed and incorporated gender, age, and PMI as covariates [21].

GSE15222. The GSE15222 dataset was used to examine eQTLs [37]. Neuropathologically confirmed AD ($n = 176$) or normal controls ($n = 188$) of self-identified individuals of European descent, were obtained from 20 National Alzheimer's Coordinating Center (NACC) brain banks and from the Miami Brain Bank. The 188 control brains came from one of three brain regions: 21% frontal cortex, 73% temporal cortex and 2% parietal cortex. The samples were 45% female with a mean age of 81 years (range 65–100) and an average post mortem interval (PMI) of 10 hours. The 176 LOAD brains were composed of 18% frontal cortex, 60% temporal cortex and 10% parietal cortex. The samples were 50% female with a mean age of 84 years (range 68–102) and an average PMI of 9 hours. An Affymetrix 500K chip was used to obtain genotype data, and an Illumina ref-seq 8 chip was used to obtain RNA expression data. To analyze RNA expression, residual values were used that were log transformed and then gender, *APOE* genotype, age, hybridization date, site, and PMI were included as covariates.

GSE5281. The GSE5281 dataset was obtained from laser microdissected neurons from AD and control brains [38]. Brain samples from 47 individuals of European descent that were collected from Washington University, Duke University, and Sun Health Research Institute were included in the study. Samples were clinically and neuropathologically confirmed AD or controls. The 33 AD samples were 54.5% female with a mean age of 79.9 years (range 73–86.8)

and an average PMI of 2.5 hours. The 14 control brains were 28.6% female with a mean age of 79.8 years (range 70.1–88.9). All samples were obtained from the entorhinal cortex, hippocampus, medial temporal gyrus, posterior cingulate, superior frontal gyrus, and primary visual cortex. RNA expression was measured using an Affymetrix GeneChip for gene expression. To analyze RNA expression, the log transformed expression values were analyzed with brain region, age, and gender as covariates.

UKBEC. The UKBEC (www.braineac.org) dataset is composed of brains from 134 neuropathologically normal controls [20]. Ten brain regions were extracted for each brain: occipital cortex (OCTX), frontal cortex (FCTX), temporal cortex (TCTX), hippocampus (HIPPI), intra-ocular white matter (WHMT), cerebellar cortex (CRBL), thalamus (THAL), putamen (PUTM), substantia nigra (SNIG), and medulla (MEDU). RNA expression was measured using an Affymetrix Exon 1.0 ST array. Genotyping was performed on the Illumina Infinium Omni1-Quad BeadChip.

IGAP LOAD GWAS

International Genomics of Alzheimer's Project (IGAP) is a large two-stage study based upon genome-wide association studies (GWAS) on individuals of European ancestry. In stage 1, IGAP used genotyped and imputed data on 7,055,881 single nucleotide polymorphisms (SNPs) to meta-analyze four previously-published GWAS datasets consisting of 17,008 Alzheimer's disease cases and 37,154 controls (The European Alzheimer's disease Initiative–EADI the Alzheimer Disease Genetics Consortium–ADGC The Cohorts for Heart and Aging Research in Genomic Epidemiology consortium–CHARGE The Genetic and Environmental Risk in AD consortium–GERAD). In stage 2, 11,632 SNPs were genotyped and tested for association in an independent set of 8,572 Alzheimer's disease cases and 11,312 controls. Finally, a meta-analysis was performed combining results from stages 1 & 2.

ADGC

The ADGC case-control database was previously described [8]. The 15 datasets with imputed data were analyzed (1,000 Genomes Project Phase 1 March 2012 v3).

Statistical analysis

Relative gene expression values were log transformed to achieve a normal distribution. To identify covariates that influence the expression of each gene, a stepwise discriminant analysis was performed using CDR, age, gender, disease status, PMI (post mortem interval), RIN (RNA integrity number), and *APOE* genotype. After applying the appropriate covariates to the model, analysis of covariance (ANCOVA) was used to test for association between genotypes and gene expression. SNPs were tested using an additive model. All analyses were performed using statistical analysis software (SAS). Conditional analyses were performed by adjusting for the most significant eQTL SNP within each IGAP GWAS locus to determine whether the eQTL SNP represented an independent association. Additional covariates included in the analyses were age, gender, principal components 1–3, and site.

Supporting Information

S1 Fig. No correlation is observed between PILRA, PILRB, and GATS in human brains.

Expression of PILRA, PILRB, and GATS were plotted in laser microdissected neurons. (PDF)

S1 Table. RegulomeDB Scores.

(XLSX)

S2 Table. eQTLs of IGAP GWAS SNPs in control brains (UKBEC).

(XLSX)

S3 Table. Most Significant eQTLs for top IGAP SNPs.

(XLSX)

S4 Table. eQTLs of genes within IGAP GWAS loci in control brains (GSE15745).

(XLSX)

S5 Table. Linkage Disequilibrium of SNPs Analyzed in GSE15222 and GSE15745.

(XLSX)

S6 Table. eQTLs of IGAP GWAS SNPs in GSE15222.

(XLSX)

S7 Table. Most significant eQTLs in IGAP loci in control brains (UKBEC).

(XLSX)

S8 Table. Top eQTLs for SNPs within IGAP Loci in Control Brains (UKBEC).

(XLSX)

S9 Table. Conditional analysis of SNPs producing the most significant eQTLs in control brains.

(XLSX)

S10 Table. Expression of IGAP GWAS loci is associated with disease status in GSE5281.

(XLSX)

S11 Table. Cell-type specific expression of genes within the IGAP GWAS loci.

(XLSX)

Acknowledgments

Funding was provided by NIH-AG035083 (AMG), NIH-AG049508 (AMG) NIH-AG046374 (CMK), and the Barnes Jewish Foundation (AMG). This work was supported by access to equipment made possible by the Hope Center for Neurological Disorders, and the Departments of Neurology and Psychiatry at Washington University School of Medicine.

We thank the International Genomics of Alzheimer's Project (IGAP) for providing summary results data for these analyses. The investigators within IGAP contributed to the design and implementation of IGAP and/or provided data but did not participate in analysis or writing of this report. IGAP was made possible by the generous participation of the control subjects, the patients, and their families. The i-Select chips was funded by the French National Foundation on Alzheimer's disease and related disorders. EADI was supported by the LABEX (laboratory of excellence program investment for the future) DISTALZ grant, Inserm, Institut Pasteur de Lille, Université de Lille 2 and the Lille University Hospital. GERAD was supported by the Medical Research Council (Grant n° 503480), Alzheimer's Research UK (Grant n° 503176), the Wellcome Trust (Grant n° 082604/2/07/Z) and German Federal Ministry of Education and Research (BMBF): Competence Network Dementia (CND) grant n° 01GI0102, 01GI0711, 01GI0420. CHARGE was partly supported by the NIH/NIA grant R01 AG033193 and the NIA AG081220 and AGES contract N01-AG-12100, the NHLBI grant R01 HL105756, the Icelandic Heart Association, and the Erasmus Medical Center and Erasmus

University. ADGC was supported by the NIH/NIA grants: U01 AG032984, U24 AG021886, U01 AG016976, and the Alzheimer's Association grant ADGC-10-196728.

The National Institutes of Health, National Institute on Aging (NIH-NIA) supported this work through the following grants: ADGC, U01 AG032984, RC2 AG036528; Samples from the National Cell Repository for Alzheimer's Disease (NCRAD), which receives government support under a cooperative agreement grant (U24 AG21886) awarded by the National Institute on Aging (NIA), were used in this study. We thank contributors who collected samples used in this study, as well as patients and their families, whose help and participation made this work possible; Data for this study were prepared, archived, and distributed by the National Institute on Aging Alzheimer's Disease Data Storage Site (NIAGADS) at the University of Pennsylvania (U24-AG041689-01); NACC, U01 AG016976; NIA LOAD, U24 AG026395, R01AG041797; Banner Sun Health Research Institute P30 AG019610; Boston University, P30 AG013846, U01 AG10483, R01 CA129769, R01 MH080295, R01 AG017173, R01 AG025259, R01AG33193; Columbia University, P50 AG008702, R37 AG015473; Duke University, P30 AG028377, AG05128; Emory University, AG025688; Group Health Research Institute, UO1 AG006781, UO1 HG004610, UO1 HG006375; Indiana University, P30 AG10133; Johns Hopkins University, P50 AG005146, R01 AG020688; Massachusetts General Hospital, P50 AG005134; Mayo Clinic, P50 AG016574; Mount Sinai School of Medicine, P50 AG005138, P01 AG002219; New York University, P30 AG08051, UL1 RR029893, 5R01AG012101, 5R01AG022374, 5R01AG013616, 1RC2AG036502, 1R01AG035137; Northwestern University, P30 AG013854; Oregon Health & Science University, P30 AG008017, R01 AG026916; Rush University, P30 AG010161, R01 AG019085, R01 AG15819, R01 AG17917, R01 AG30146; TGen, R01 NS059873; University of Alabama at Birmingham, P50 AG016582; University of Arizona, R01 AG031581; University of California, Davis, P30 AG010129; University of California, Irvine, P50 AG016573; University of California, Los Angeles, P50 AG016570; University of California, San Diego, P50 AG005131; University of California, San Francisco, P50 AG023501, P01 AG019724; University of Kentucky, P30 AG028383, AG05144; University of Michigan, P50 AG008671; University of Pennsylvania, P30 AG010124; University of Pittsburgh, P50 AG005133, AG030653, AG041718, AG07562, AG02365; University of Southern California, P50 AG005142; University of Texas Southwestern, P30 AG012300; University of Miami, R01 AG027944, AG010491, AG027944, AG021547, AG019757; University of Washington, P50 AG005136; University of Wisconsin, P50 AG033514; Vanderbilt University, R01 AG019085; and Washington University, P50 AG005681, P01 AG03991. The Kathleen Price Bryan Brain Bank at Duke University Medical Center is funded by NINDS grant # NS39764, NIMH MH60451 and by Glaxo Smith Kline. Genotyping of the TGEN2 cohort was supported by Kronos Science. The TGen series was also funded by NIA grant AG041232 to AJM and MJH, The Banner Alzheimer's Foundation, The Johnnie B. Byrd Sr. Alzheimer's Institute, the Medical Research Council, and the state of Arizona and also includes samples from the following sites: Newcastle Brain Tissue Resource (funding via the Medical Research Council, local NHS trusts and Newcastle University), MRC London Brain Bank for Neurodegenerative Diseases (funding via the Medical Research Council), South West Dementia Brain Bank (funding via numerous sources including the Higher Education Funding Council for England (HEFCE), Alzheimer's Research Trust (ART), BRACE as well as North Bristol NHS Trust Research and Innovation Department and DeNDRoN), The Netherlands Brain Bank (funding via numerous sources including Stichting MS Research, Brain Net Europe, Hersenstichting Nederland Breinbrekend Werk, International Parkinson Fonds, Internationale Stichting Alzheimer Onderzoek), Institut de Neuropatologia, Servei Anatomia Patologica, Universitat de Barcelona. ADNI data collection and sharing was funded by the National Institutes of Health Grant U01 AG024904 and Department of Defense award number W81XWH-12-2-0012. ADNI is funded by the National

Institute on Aging, the National Institute of Biomedical Imaging and Bioengineering, and through generous contributions from the following: AbbVie, Alzheimer's Association; Alzheimer's Drug Discovery Foundation; Araclon Biotech; BioClinica, Inc.; Biogen; Bristol-Myers Squibb Company; CereSpir, Inc.; Eisai Inc.; Elan Pharmaceuticals, Inc.; Eli Lilly and Company; EuroImmun; F. Hoffmann-La Roche Ltd and its affiliated company Genentech, Inc.; Fujirebio; GE Healthcare; IXICO Ltd.; Janssen Alzheimer Immunotherapy Research & Development, LLC.; Johnson & Johnson Pharmaceutical Research & Development LLC.; Lumosity; Lundbeck; Merck & Co., Inc.; Meso Scale Diagnostics, LLC.; NeuroRx Research; Neurotrack Technologies; Novartis Pharmaceuticals Corporation; Pfizer Inc.; Piramal Imaging; Servier; Takeda Pharmaceutical Company; and Transition Therapeutics. The Canadian Institutes of Health Research is providing funds to support ADNI clinical sites in Canada. Private sector contributions are facilitated by the Foundation for the National Institutes of Health (www.fnih.org). The grantee organization is the Northern California Institute for Research and Education, and the study is coordinated by the Alzheimer's Disease Cooperative Study at the University of California, San Diego. ADNI data are disseminated by the Laboratory for Neuro Imaging at the University of Southern California. We thank Drs. D. Stephen Snyder and Marilyn Miller from NIA who are *ex-officio* ADGC members. Support was also from the Alzheimer's Association (LAF, IIRG-08-89720; MP-V, IIRG-05-14147) and the US Department of Veterans Affairs Administration, Office of Research and Development, Biomedical Laboratory Research Program. P.S.G.-H. is supported by Wellcome Trust, Howard Hughes Medical Institute, and the Canadian Institute of Health Research.

The members of the Alzheimer's Disease Genetics Consortium are: Marilyn S. Albert¹, Roger L. Albin^{2,3}, Liana G. Apostolova⁴, Steven E. Arnold⁵, Clinton T. Baldwin⁶, Robert Barber⁷, Michael M. Barmada⁸, Lisa L. Barnes^{9,10}, Thomas G. Beach¹¹, Gary W. Beecham^{12,13}, Duane Beekly¹⁴, David A. Bennett^{9,15}, Eileen H. Bigio¹⁶, Thomas D. Bird¹⁷, Deborah Blacker^{18,19}, Bradley F. Boeve²⁰, James D. Bowen²¹, Adam Boxer²², James R. Burke²³, Joseph D. Buxbaum²⁴⁻²⁶, Nigel J. Cairns²⁷, Laura B. Cantwell²⁸, Chuanhai Cao²⁹, Chris S. Carlson³⁰, Regina M. Carney³¹, Minerva M. Carrasquillo³², Steven L. Carroll³³, Helena C. Chui³⁴, David G. Clark³⁵, Jason Corneveaux³⁶, Paul K. Crane³⁷, David H. Cribbs³⁸, Elizabeth A. Crocco³⁹, Carlos Cruchaga⁴⁰, Philip L. De Jager^{41,42}, Charles DeCarli⁴³, Steven T. DeKosky⁴⁴, F. Yesim Demirci⁸, Malcolm Dick⁴⁵, Dennis W. Dickson³², Ranjan Duara⁴⁶, Nilufer Ertekin-Taner^{32,47}, Denis Evans⁴⁸, Kelley M. Faber⁴⁹, Kenneth B. Fallon³³, Martin R. Farlow⁵⁰, Steven Ferris⁵¹, Tatiana M. Foroud⁴⁹, Matthew P. Frosch⁵², Douglas R. Galasko⁵³, Mary Ganguli⁵⁴, Marla Gearing^{55,56}, Daniel H. Geschwind⁵⁷, Bernardino Ghetti⁵⁸, John R. Gilbert^{12,13}, Sid Gilman², Jonathan D. Glass⁵⁹, Alison M. Goate⁴⁰, Neill R. Graff-Radford^{32,47}, Robert C. Green⁶⁰, John H. Growdon⁶¹, Hakon Hakonarson⁶², Kara L. Hamilton-Nelson¹², Ronald L. Hamilton⁶³, John Hardy⁶⁴, Lindy E. Harrell³⁵, Elizabeth Head⁶⁵, Lawrence S. Honig⁶⁶, Matthew J. Huentelman³⁶, Christine M. Hulette⁶⁷, Bradley T. Hyman⁶¹, Gail P. Jarvik^{68,69}, Gregory A. Jicha⁷⁰, Lee-Way Jin⁷¹, M. Ilyas Kamboh^{8,72}, Anna Karydas²², John S.K. Kauwe⁷³, Jeffrey A. Kaye^{74,75}, Ronald Kim⁷⁶, Edward H. Koo⁵³, Neil W. Kowall^{77,78}, Joel H. Kramer⁷⁹, Patricia Kramer^{74,80}, Walter A. Kukull⁸¹, Frank M. LaFerla⁸², James J. Lah⁵⁹, Eric B. Larson^{37,83}, James B. Leverenz⁸⁴, Allan I. Levey⁵⁹, Ge Li⁸⁵, Chiao-Feng Lin²⁸, Andrew P. Lieberman⁸⁶, Oscar L. Lopez⁷², Kathryn L. Lunetta⁸⁷, Constantine G. Lyketsos⁸⁸, Wendy J. Mack⁸⁹, Daniel C. Marson³⁵, Eden R. Martin^{12,13}, Frank Martiniuk⁹⁰, Deborah C. Mash⁹¹, Eliezer Masliah^{53,92}, Wayne C. McCormick³⁷, Susan M. McCurry⁹³, Andrew N. McDavid³⁰, Ann C. McKee^{77,78}, Marsel Mesulam⁹⁴, Bruce L. Miller²², Carol A. Miller⁹⁵, Joshua W. Miller⁷¹, Thomas J. Montine⁸⁴, John C. Morris^{27,96}, Jill R. Murrell^{49,58}, Amanda J. Myers³⁹, Adam C. Naj¹², John M. Olichney⁴³, Vernon S. Pankratz⁹⁷, Joseph E. Parisi^{98,99}, Elaine Peskind⁸⁵, Ronald C. Petersen²⁰, Aimee Pierce³⁸, Wayne W. Poon⁴⁵, Huntington Potter²⁹, Joseph F. Quinn⁷⁴, Ashok Raj²⁹, Ruchita A. Rajbhandary¹²,

Murray Raskind⁸⁵, Eric M. Reiman^{36,100–102}, Barry Reisberg^{51,103}, Christiane Reitz^{66,104,105}, John M. Ringman⁴, Erik D. Roberson³⁵, Ekaterina Rogaeva¹⁰⁶, Howard J. Rosen²², Roger N. Rosenberg¹⁰⁷, Mary Sano²⁵, Andrew J. Saykin^{49,108}, Julie A. Schneider^{9,109}, Lon S. Schneider^{34,110}, William W. Seeley²², Amanda G. Smith²⁹, Joshua A. Sonnen⁸⁴, Salvatore Spina⁵⁸, Robert A. Stern⁷⁷, Rudolph E. Tanzi⁶¹, John Q. Trojanowski²⁸, Juan C. Troncoso¹¹¹, Debby W. Tsuang⁸⁵, Otto Valladares²⁸, Vivianna M. Van Deerlin²⁸, Linda J. Van Eldik¹¹², Badri N. Vardarajan⁶, Harry V. Vinters^{4,113}, Jean Paul Vonsattel¹¹⁴, Sandra Weintraub⁹⁴, Kathleen A. Welsh-Bohmer^{23,115}, Jennifer Williamson⁶⁶, Randall L. Woltjer¹¹⁶, Clinton B. Wright¹¹⁷, Steven G. Younkin³², Chang-En Yu³⁷, Lei Yu⁹.

1 Department of Neurology, Johns Hopkins University, Baltimore, Maryland.

2 Department of Neurology, University of Michigan, Ann Arbor, Michigan.

3 Geriatric Research, Education and Clinical Center (GRECC), VA Ann Arbor Healthcare System (VAAHS), Ann Arbor, Michigan.

4 Department of Neurology, University of California Los Angeles, Los Angeles, California.

5 Department of Psychiatry, University of Pennsylvania Perelman School of Medicine, Philadelphia, Pennsylvania.

6 Department of Medicine (Genetics Program), Boston University, Boston, Massachusetts.

7 Department of Pharmacology and Neuroscience, University of North Texas Health Science Center, Fort Worth, Texas.

8 Department of Human Genetics, University of Pittsburgh, Pittsburgh, Pennsylvania.

9 Department of Neurological Sciences, Rush University Medical Center, Chicago, Illinois.

10 Department of Behavioral Sciences, Rush University Medical Center, Chicago, Illinois.

11 Civil Laboratory for Neuropathology, Banner Sun Health Research Institute, Phoenix, Arizona.

12 The John P. Hussman Institute for Human Genomics, University of Miami, Miami, Florida.

13 Dr. John T. Macdonald Foundation Department of Human Genetics, University of Miami, Miami, Florida.

14 National Alzheimer's Coordinating Center, University of Washington, Seattle, Washington.

15 Rush Alzheimer's Disease Center, Rush University Medical Center, Chicago, Illinois.

16 Department of Pathology, Northwestern University, Chicago, Illinois.

17 Department of Neurology, University of Washington, Seattle, Washington.

18 Department of Epidemiology, Harvard School of Public Health, Boston, Massachusetts.

19 Department of Psychiatry, Massachusetts General Hospital/Harvard Medical School, Boston, Massachusetts.

20 Department of Neurology, Mayo Clinic, Rochester, Minnesota.

21 Swedish Medical Center, Seattle, Washington.

22 Department of Neurology, University of California San Francisco, San Francisco, California.

23 Department of Medicine, Duke University, Durham, North Carolina.

24 Department of Neuroscience, Mount Sinai School of Medicine, New York.

25 Department of Psychiatry, Mount Sinai School of Medicine, New York.

26 Departments of Genetics and Genomic Sciences, Mount Sinai School of Medicine, New York.

27 Department of Pathology and Immunology, Washington University, St. Louis, Missouri.

28 Department of Pathology and Laboratory Medicine, University of Pennsylvania Perelman School of Medicine, Philadelphia, Pennsylvania.

29 USF Health Byrd Alzheimer's Institute, University of South Florida, Tampa, Florida.

- 30 Fred Hutchinson Cancer Research Center, Seattle, Washington.
- 31 Department of Psychiatry, Vanderbilt University, Nashville, Tennessee.
- 32 Department of Neuroscience, Mayo Clinic, Jacksonville, Florida.
- 33 Department of Pathology, University of Alabama at Birmingham, Birmingham, Alabama.
- 34 Department of Neurology, University of Southern California, Los Angeles, California.
- 35 Department of Neurology, University of Alabama at Birmingham, Birmingham, Alabama.
- 36 Neurogenomics Division, Translational Genomics Research Institute, Phoenix, Arizona.
- 37 Department of Medicine, University of Washington, Seattle, Washington.
- 38 Department of Neurology, University of California Irvine, Irvine, California.
- 39 Department of Psychiatry and Behavioral Sciences, Miller School of Medicine, University of Miami, Miami, Florida.
- 40 Department of Psychiatry and Hope Center Program on Protein Aggregation and Neurodegeneration, Washington University School of Medicine, St. Louis, Missouri.
- 41 Program in Translational NeuroPsychiatric Genomics, Institute for the Neurosciences, Department of Neurology & Psychiatry, Brigham and Women's Hospital and Harvard Medical School, Boston, Massachusetts.
- 42 Program in Medical and Population Genetics, Broad Institute, Cambridge, Massachusetts.
- 43 Department of Neurology, University of California Davis, Sacramento, California.
- 44 University of Virginia School of Medicine, Charlottesville, Virginia.
- 45 Institute for Memory Impairments and Neurological Disorders, University of California Irvine, Irvine, California.
- 46 Wien Center for Alzheimer's Disease and Memory Disorders, Mount Sinai Medical Center, Miami Beach, Florida.
- 47 Department of Neurology, Mayo Clinic, Jacksonville, Florida.
- 48 Rush Institute for Healthy Aging, Department of Internal Medicine, Rush University Medical Center, Chicago, Illinois.
- 49 Department of Medical and Molecular Genetics, Indiana University, Indianapolis, Indiana.
- 50 Department of Neurology, Indiana University, Indianapolis, Indiana.
- 51 Department of Psychiatry, New York University, New York.
- 52 C.S. Kubik Laboratory for Neuropathology, Massachusetts General Hospital, Charlestown, Massachusetts.
- 53 Department of Neurosciences, University of California San Diego, La Jolla, California.
- 54 Department of Psychiatry, University of Pittsburgh, Pittsburgh, Pennsylvania.
- 55 Department of Pathology and Laboratory Medicine, Emory University, Atlanta, Georgia.
- 56 Emory Alzheimer's Disease Center, Emory University, Atlanta, Georgia.
- 57 Neurogenetics Program, University of California Los Angeles, Los Angeles, California.
- 58 Department of Pathology and Laboratory Medicine, Indiana University, Indianapolis, Indiana.
- 59 Department of Neurology, Emory University, Atlanta, Georgia.
- 60 Division of Genetics, Department of Medicine and Partners Center for Personalized Genetic Medicine, Brigham and Women's Hospital and Harvard Medical School, Boston, Massachusetts.
- 61 Department of Neurology, Massachusetts General Hospital/Harvard Medical School, Boston, Massachusetts.

- 62 Center for Applied Genomics, Children's Hospital of Philadelphia, Philadelphia, Pennsylvania.
- 63 Department of Pathology (Neuropathology), University of Pittsburgh, Pittsburgh, Pennsylvania.
- 64 Institute of Neurology, University College London, Queen Square, London.
- 65 Sanders-Brown Center on Aging, Department of Molecular and Biomedical Pharmacology, University of Kentucky, Lexington, Kentucky.
- 66 Taub Institute on Alzheimer's Disease and the Aging Brain, Department of Neurology, Columbia University, New York.
- 67 Department of Pathology, Duke University, Durham, North Carolina.
- 68 Department of Genome Sciences, University of Washington, Seattle, Washington.
- 69 Department of Medicine (Medical Genetics), University of Washington, Seattle, Washington.
- 70 Sanders-Brown Center on Aging, Department Neurology, University of Kentucky, Lexington, Kentucky.
- 71 Department of Pathology and Laboratory Medicine, University of California Davis, Sacramento, California.
- 72 University of Pittsburgh Alzheimer's Disease Research Center, Pittsburgh, Pennsylvania.
- 73 Department of Biology, Brigham Young University, Provo, Utah.
- 74 Department of Neurology, Oregon Health & Science University, Portland, Oregon.
- 75 Department of Neurology, Portland Veterans Affairs Medical Center, Portland, Oregon.
- 76 Department of Pathology and Laboratory Medicine, University of California Irvine, Irvine, California.
- 77 Department of Neurology, Boston University, Boston, Massachusetts.
- 78 Department of Pathology, Boston University, Boston, Massachusetts.
- 79 Department of Neuropsychology, University of California San Francisco, San Francisco, California.
- 80 Department of Molecular & Medical Genetics, Oregon Health & Science University, Portland, Oregon.
- 81 Department of Epidemiology, University of Washington, Seattle, Washington.
- 82 Department of Neurobiology and Behavior, University of California Irvine, Irvine, California.
- 83 Group Health Research Institute, Group Health, Seattle, Washington.
- 84 Department of Pathology, University of Washington, Seattle, Washington.
- 85 Department of Psychiatry and Behavioral Sciences, University of Washington, Seattle, Washington.
- 86 Department of Pathology, University of Michigan, Ann Arbor, Michigan.
- 87 Department of Biostatistics, Boston University, Boston, Massachusetts.
- 88 Department of Psychiatry, Johns Hopkins University, Baltimore, Maryland.
- 89 Department of Preventive Medicine, University of Southern California, Los Angeles, California.
- 90 Department of Medicine—Pulmonary, New York University, New York.
- 91 Department of Neurology, University of Miami, Miami, Florida.
- 92 Department of Pathology, University of California San Diego, La Jolla, California.
- 93 School of Nursing Northwest Research Group on Aging, University of Washington, Seattle, Washington.
- 94 Cognitive Neurology and Alzheimer's Disease Center, Northwestern University, Chicago, Illinois.
- 95 Department of Pathology, University of Southern California, Los Angeles, California.

- 96 Department of Neurology, Washington University, St. Louis, Missouri.
97 Department of Biostatistics, Mayo Clinic, Rochester, Minnesota.
98 Department of Anatomic Pathology, Mayo Clinic, Rochester, Minnesota.
99 Department of Laboratory Medicine and Pathology, Mayo Clinic, Rochester, Minnesota.
100 Arizona Alzheimer's Consortium, Phoenix, Arizona.
101 Banner Alzheimer's Institute, Phoenix, Arizona.
102 Department of Psychiatry, University of Arizona, Phoenix, Arizona.
103 Alzheimer's Disease Center, New York University, New York.
104 Gertrude H. Sergievsky Center, Columbia University, New York.
105 Department of Neurology, Columbia University, New York.
106 Tanz Centre for Research in Neurodegenerative Disease, University of Toronto, Toronto, Ontario.
107 Department of Neurology, University of Texas Southwestern, Dallas, Texas.
108 Department of Radiology and Imaging Sciences, Indiana University, Indianapolis, Indiana.
109 Department of Pathology (Neuropathology), Rush University Medical Center, Chicago, Illinois.
110 Department of Psychiatry, University of Southern California, Los Angeles, California.
111 Department of Pathology, Johns Hopkins University, Baltimore, Maryland.
112 Sanders-Brown Center on Aging, Department of Anatomy and Neurobiology, University of Kentucky, Lexington, Kentucky.
113 Department of Pathology & Laboratory Medicine, University of California Los Angeles, Los Angeles, California.
114 Taub Institute on Alzheimer's Disease and the Aging Brain, Department of Pathology, Columbia University, New York.
115 Department of Psychiatry & Behavioral Sciences, Duke University, Durham, North Carolina.
116 Department of Pathology, Oregon Health & Science University, Portland, Oregon.
117 Evelyn F. McKnight Brain Institute, Department of Neurology, Miller School of Medicine, University of Miami, Miami, Florida.

Author Contributions

Conceived and designed the experiments: CMK AMG. Performed the experiments: CMK LAE SB. Analyzed the data: CMK LAE SB. Contributed reagents/materials/analysis tools: ADGC. Wrote the paper: CMK AMG.

References

1. Karch CM, Cruchaga C, Goate AM. Alzheimer's disease genetics: from the bench to the clinic. *Neuron*. 2014; 83(1):11–26. doi: [10.1016/j.neuron.2014.05.041](https://doi.org/10.1016/j.neuron.2014.05.041) PMID: [24991952](https://pubmed.ncbi.nlm.nih.gov/24991952/); PubMed Central PMCID: PMC4120741.
2. Guerreiro RJ, Gustafson DR, Hardy J. The genetic architecture of Alzheimer's disease: beyond APP, PSENs and APOE. *Neurobiol Aging*. 2012; 33(3):437–56. Epub 2010/07/03. doi: [10.1016/j.neurobiolaging.2010.03.025](https://doi.org/10.1016/j.neurobiolaging.2010.03.025) PMID: [20594621](https://pubmed.ncbi.nlm.nih.gov/20594621/); PubMed Central PMCID: PMC2980860.
3. Bertram L, Lange C, Mullin K, Parkinson M, Hsiao M, Hogan MF, et al. Genome-wide association analysis reveals putative Alzheimer's disease susceptibility loci in addition to APOE. *Am J Hum Genet*. 2008; 83(5):623–32. Epub 2008/11/04. doi: [10.1016/j.ajhg.2008.10.008](https://doi.org/10.1016/j.ajhg.2008.10.008) PMID: [18976728](https://pubmed.ncbi.nlm.nih.gov/18976728/); PubMed Central PMCID: PMC2668052.
4. Harold D, Abraham R, Hollingworth P, Sims R, Gerrish A, Hamshere ML, et al. Genome-wide association study identifies variants at *CLU* and *PICALM* associated with Alzheimer's disease. *Nat Genet*. 2009; 41(10):1088–93. PMID: [19734902](https://pubmed.ncbi.nlm.nih.gov/19734902/). doi: [10.1038/ng.440](https://doi.org/10.1038/ng.440)

5. Lambert J-C, Heath S, Even G, Campion D, Sleegers K, Hiltunen M, et al. Genome-wide association study identifies variants at *CLU* and *CR1* associated with Alzheimer's disease. *Nat Genet.* 2009; 41(10):1094–9. PMID: [19734903](#). doi: [10.1038/ng.439](#)
6. Seshadri S, Fitzpatrick AL, Ikram MA, DeStefano AL, Gudnason V, Boada M, et al. Genome-wide analysis of genetic loci associated with Alzheimer disease. *Jama.* 2010; 303(18):1832–40. Epub 2010/05/13. doi: [10.1001/jama.2010.574](#) PMID: [20460622](#); PubMed Central PMCID: PMC2989531.
7. Hollingworth P, Harold D, Sims R, Gerrish A, Lambert J-C, Carrasquillo MM, et al. Common variants at *ABCA7*, *MS4A6A/MS4A4E*, *EPHA1*, *CD33* and *CD2AP* are associated with Alzheimer's disease. *Nat Genet.* 2011; 43(5):429–35. PMID: [21460840](#). doi: [10.1038/ng.803](#)
8. Naj AC, Jun G, Beecham GW, Wang L-S, Vardarajan BN, Buross J, et al. Common variants at *MS4A4/MS4A6E*, *CD2AP*, *CD33* and *EPHA1* are associated with late-onset Alzheimer's disease. *Nat Genet.* 2011; 43(5):436–41. PMID: [21460841](#). doi: [10.1038/ng.801](#)
9. Lambert JC, Ibrahim-Verbaas CA, Harold D, Naj AC, Sims R, Bellenguez C, et al. Meta-analysis of 74,046 individuals identifies 11 new susceptibility loci for Alzheimer's disease. *Nat Genet.* 2013. Epub 2013/10/29. doi: [10.1038/ng.2802](#) PMID: [24162737](#).
10. Escott-Price V, Bellenguez C, Wang LS, Choi SH, Harold D, Jones L, et al. Gene-wide analysis detects two new susceptibility genes for Alzheimer's disease. *PLoS One.* 2014; 9(6):e94661. doi: [10.1371/journal.pone.0094661](#) PMID: [24922517](#); PubMed Central PMCID: PMC4055488.
11. Griciuc A, Serrano-Pozo A, Parrado AR, Lesinski AN, Asselin CN, Mullin K, et al. Alzheimer's disease risk gene *CD33* inhibits microglial uptake of amyloid beta. *Neuron.* 2013; 78(4):631–43. Epub 2013/04/30. doi: [10.1016/j.neuron.2013.04.014](#) PMID: [23623698](#); PubMed Central PMCID: PMC3706457.
12. Xiao Q, Gil SC, Yan P, Wang Y, Han S, Gonzales E, et al. Role of phosphatidylinositol clathrin assembly lymphoid-myeloid leukemia (*PICALM*) in intracellular amyloid precursor protein (*APP*) processing and amyloid plaque pathogenesis. *J Biol Chem.* 2012; 287(25):21279–89. Epub 2012/04/28. doi: [10.1074/jbc.M111.338376](#) PMID: [22539346](#); PubMed Central PMCID: PMC3375549.
13. Chapuis J, Hansmannel F, Gistelinc M, Mounier A, Van Cauwenberghe C, Kolen KV, et al. Increased expression of *BIN1* mediates Alzheimer genetic risk by modulating tau pathology. *Mol Psychiatry.* 2013; 18(11):1225–34. Epub 2013/02/13. doi: [10.1038/mp.2013.1](#) PMID: [23399914](#); PubMed Central PMCID: PMC3807661.
14. Malik M, Simpson JF, Parikh I, Wilfred BR, Fardo DW, Nelson PT, et al. *CD33* Alzheimer's risk-altering polymorphism, *CD33* expression, and exon 2 splicing. *J Neurosci.* 2013; 33(33):13320–5. Epub 2013/08/16. doi: [10.1523/JNEUROSCI.1224-13.2013](#) PMID: [23946390](#); PubMed Central PMCID: PMC3742922.
15. Karch CM, Jeng AT, Nowotny P, Cady J, Cruchaga C, Goate AM. Expression of novel Alzheimer's disease risk genes in control and Alzheimer's disease brains. *PLoS One.* 2012; 7(11):e50976. Epub 2012/12/12. doi: [10.1371/journal.pone.0050976](#) PMID: [23226438](#); PubMed Central PMCID: PMC3511432.
16. Allen M, Zou F, Chai HS, Younkin CS, Crook J, Pankratz VS, et al. Novel late-onset Alzheimer disease loci variants associate with brain gene expression. *Neurology.* 2012; 79(3):221–8. Epub 2012/06/23. doi: [10.1212/WNL.0b013e3182605801](#) PMID: [22722634](#); PubMed Central PMCID: PMC3398432.
17. Holton P, Ryten M, Nalls M, Trabzuni D, Weale ME, Hernandez D, et al. Initial assessment of the pathogenic mechanisms of the recently identified Alzheimer risk Loci. *Ann Hum Genet.* 2013; 77(2):85–105. doi: [10.1111/ahg.12000](#) PMID: [23360175](#); PubMed Central PMCID: PMC3578142.
18. Boyle AP, Hong EL, Hariharan M, Cheng Y, Schaub MA, Kasowski M, et al. Annotation of functional variation in personal genomes using RegulomeDB. *Genome research.* 2012; 22(9):1790–7. doi: [10.1101/gr.137323.112](#) PMID: [22955989](#); PubMed Central PMCID: PMC3431494.
19. Rosenthal SL, Barmada MM, Wang X, Demirci FY, Kamboh MI. Connecting the dots: potential of data integration to identify regulatory SNPs in late-onset Alzheimer's disease GWAS findings. *PLoS One.* 2014; 9(4):e95152. doi: [10.1371/journal.pone.0095152](#) PMID: [24743338](#); PubMed Central PMCID: PMC3990600.
20. Ramasamy A, Trabzuni D, Guelfi S, Varghese V, Smith C, Walker R, et al. Genetic variability in the regulation of gene expression in ten regions of the human brain. *Nat Neurosci.* 2014; 17(10):1418–28. doi: [10.1038/nn.3801](#) PMID: [25174004](#).
21. Gibbs JR, van der Brug MP, Hernandez DG, Traynor BJ, Nalls MA, Lai SL, et al. Abundant quantitative trait loci exist for DNA methylation and gene expression in human brain. *PLoS Genet.* 2010; 6(5):e1000952. doi: [10.1371/journal.pgen.1000952](#) PMID: [20485568](#); PubMed Central PMCID: PMC2869317.
22. Zou F, Chai HS, Younkin CS, Allen M, Crook J, Pankratz VS, et al. Brain expression genome-wide association study (eGWAS) identifies human disease-associated variants. *PLoS Genet.* 2012; 8(6):e1002707. doi: [10.1371/journal.pgen.1002707](#) PMID: [22685416](#); PubMed Central PMCID: PMC3369937.

23. Zhang Y, Chen K, Sloan SA, Bennett ML, Scholze AR, O'Keefe S, et al. An RNA-Sequencing Transcriptome and Splicing Database of Glia, Neurons, and Vascular Cells of the Cerebral Cortex. *J Neurosci*. 2014; 34(36):11929–47. doi: [10.1523/JNEUROSCI.1860-14.2014](https://doi.org/10.1523/JNEUROSCI.1860-14.2014) PMID: [25186741](https://pubmed.ncbi.nlm.nih.gov/25186741/); PubMed Central PMCID: PMC4152602.
24. Mousseau DD, Banville D, L'Abbe D, Bouchard P, Shen SH. PILRalpha, a novel immunoreceptor tyrosine-based inhibitory motif-bearing protein, recruits SHP-1 upon tyrosine phosphorylation and is paired with the truncated counterpart PILRbeta. *J Biol Chem*. 2000; 275(6):4467–74. PMID: [10660620](https://pubmed.ncbi.nlm.nih.gov/10660620/).
25. Wunderlich P, Glebov K, Kemmerling N, Tien NT, Neumann H, Walter J. Sequential proteolytic processing of the triggering receptor expressed on myeloid cells-2 (TREM2) by ectodomain shedding and gamma-secretase dependent intramembranous cleavage. *J Biol Chem*. 2013. Epub 2013/10/01. doi: [10.1074/jbc.M113.517540](https://doi.org/10.1074/jbc.M113.517540) PMID: [24078628](https://pubmed.ncbi.nlm.nih.gov/24078628/).
26. Guerreiro R, Wojtas A, Bras J, Carrasquillo M, Rogaeva E, Majounie E, et al. TREM2 variants in Alzheimer's disease. *N Engl J Med*. 2013; 368(2):117–27. Epub 2012/11/16. doi: [10.1056/NEJMoa1211851](https://doi.org/10.1056/NEJMoa1211851) PMID: [23150934](https://pubmed.ncbi.nlm.nih.gov/23150934/); PubMed Central PMCID: PMC3631573.
27. Colonna M. TREMs in the immune system and beyond. *Nat Rev Immunol*. 2003; 3(6):445–53. Epub 2003/05/31. doi: [10.1038/nri1106](https://doi.org/10.1038/nri1106) PMID: [12776204](https://pubmed.ncbi.nlm.nih.gov/12776204/).
28. Shiratori I, Ogasawara K, Saito T, Lanier LL, Arase H. Activation of natural killer cells and dendritic cells upon recognition of a novel CD99-like ligand by paired immunoglobulin-like type 2 receptor. *J Exp Med*. 2004; 199(4):525–33. doi: [10.1084/jem.20031885](https://doi.org/10.1084/jem.20031885) PMID: [14970179](https://pubmed.ncbi.nlm.nih.gov/14970179/); PubMed Central PMCID: PMC2211832.
29. Lu Q, Lu G, Qi J, Wang H, Xuan Y, Wang Q, et al. PILRalpha and PILRbeta have a siglec fold and provide the basis of binding to sialic acid. *Proc Natl Acad Sci U S A*. 2014; 111(22):8221–6. doi: [10.1073/pnas.1320716111](https://doi.org/10.1073/pnas.1320716111) PMID: [24843130](https://pubmed.ncbi.nlm.nih.gov/24843130/); PubMed Central PMCID: PMC4050567.
30. Zeller T, Wild P, Szymczak S, Rotival M, Schillert A, Castagne R, et al. Genetics and beyond—the transcriptome of human monocytes and disease susceptibility. *PLoS One*. 2010; 5(5):e10693. doi: [10.1371/journal.pone.0010693](https://doi.org/10.1371/journal.pone.0010693) PMID: [20502693](https://pubmed.ncbi.nlm.nih.gov/20502693/); PubMed Central PMCID: PMC2872668.
31. Katz C, Zaltsman-Amir Y, Mostizky Y, Kollet N, Gross A, Friedler A. Molecular basis of the interaction between proapoptotic truncated BID (tBID) protein and mitochondrial carrier homologue 2 (MTCH2) protein: key players in mitochondrial death pathway. *J Biol Chem*. 2012; 287(18):15016–23. doi: [10.1074/jbc.M111.328377](https://doi.org/10.1074/jbc.M111.328377) PMID: [22416135](https://pubmed.ncbi.nlm.nih.gov/22416135/); PubMed Central PMCID: PMC3340256.
32. Xu Xuemin S Y-c, Gao Wei, Mao Guozhang, Zhao Guojun, Agrawal Sudesh, Chisolm Guy M., Sui Dexin, and Cui Mei-Zhen The Novel Presenilin-1-associated Protein Is a Proapoptotic Mitochondrial Protein *J Biol Chem*. 2002; 277:48913–22. doi: [10.1074/jbc.M209613200](https://doi.org/10.1074/jbc.M209613200) PMID: [12377771](https://pubmed.ncbi.nlm.nih.gov/12377771/)
33. Xu X, Shi Y, Wu X, Gambetti P, Sui D, Cui MZ. Identification of a novel PSD-95/Dlg/ZO-1 (PDZ)-like protein interacting with the C terminus of presenilin-1. *J Biol Chem*. 1999; 274(46):32543–6. PMID: [10551805](https://pubmed.ncbi.nlm.nih.gov/10551805/).
34. Woulfe JM, Hammond R, Richardson B, Sooriabalan D, Parks W, Rippstein P, et al. Reduction of neuronal intranuclear rodlets immunoreactive for tubulin and glucocorticoid receptor in Alzheimer's disease. *Brain Pathol*. 2002; 12(3):300–7. PMID: [12146798](https://pubmed.ncbi.nlm.nih.gov/12146798/).
35. D'Angelo MA, Raices M, Panowski SH, Hetzer MW. Age-dependent deterioration of nuclear pore complexes causes a loss of nuclear integrity in postmitotic cells. *Cell*. 2009; 136(2):284–95. doi: [10.1016/j.cell.2008.11.037](https://doi.org/10.1016/j.cell.2008.11.037) PMID: [19167330](https://pubmed.ncbi.nlm.nih.gov/19167330/); PubMed Central PMCID: PMC2805151.
36. Raj T, Rothamel K, Mostafavi S, Ye C, Lee MN, Replogle JM, et al. Polarization of the effects of autoimmune and neurodegenerative risk alleles in leukocytes. *Science*. 2014; 344(6183):519–23. doi: [10.1126/science.1249547](https://doi.org/10.1126/science.1249547) PMID: [24786080](https://pubmed.ncbi.nlm.nih.gov/24786080/).
37. Myers AJ, Gibbs JR, Webster JA, Rohrer K, Zhao A, Marlowe L, et al. A survey of genetic human cortical gene expression. *Nat Genet*. 2007; 39(12):1494–9. PMID: [17982457](https://pubmed.ncbi.nlm.nih.gov/17982457/).
38. Liang WS, Reiman EM, Valla J, Dunkley T, Beach TG, Grover A, et al. Alzheimer's disease is associated with reduced expression of energy metabolism genes in posterior cingulate neurons. *Proc Natl Acad Sci U S A*. 2008; 105(11):4441–6. doi: [10.1073/pnas.0709259105](https://doi.org/10.1073/pnas.0709259105) PMID: [18332434](https://pubmed.ncbi.nlm.nih.gov/18332434/); PubMed Central PMCID: PMC2393743.